Andreev reflection and shot noise in a quantum dot with phonon modes

2009 J. Phys.: Condens. Matter 21 095602

(http://iopscience.iop.org/0953-8984/21/9/095602)

J. Phys.: Condens. Matter **21** (2009) 095602 (8pp) doi:10.1088/0953-8984/21/9/095602

Andreev reflection and shot noise in a quantum dot with phonon modes

Peng Zhang and Yu-xian Li

College of Physics, Hebei Normal University, Shijiazhuang 050016, People's Republic of China
and
Heibei Advanced Film Laboratory, Shijiazhuang 050016, People's Republic of China

Received 12 November 2008, in final form 30 December 2008
Published 4 February 2009
Online at stacks.iop.org/JPhysCM/21/095602

Abstract

Building on the nonequilibrium Green's function technique and a canonical transformation of the electron–phonon interaction, this paper focuses on the study of the Andreev reflection conductance and the shot noise in a single quantum dot coupling with local phonon modes. The effect of the intradot spin-flip interaction on the transport properties is considered. We pay attention to the effects of the phonon on the Andreev reflection conductance and the shot noise. It is found that splits due to spin-flip scattering appear not only in the main Andreev reflection peaks but also in the new satellite peaks. The electron–phonon interaction leads to new satellite resonant peaks that are located exactly on the integer number of the phonon frequency. Moreover, the peak height is sensitive to the electron–phonon coupling. Even if the electron–phonon coupling is weak, the shot noise spectrum shows the phonon mode peaks rather clearly, but in the Andreev reflection conductance the phonon mode peaks weakly.

1. Introduction

Modern nanotechnology has provided the possibility of fabricating nanostructures [1–4]. This has led to the exploration of electronic devices based on a single molecule, i.e. the single-molecule transistor (SMT), which provides us with a controllable tool for studying fundamental physics on the nanometer scale. It has been found that tunneling through the SMT exhibits clear many-body correlation effects at low temperature, for example, the Coulomb blockade and the Kondo effects [5–9]. Since single molecules have much smaller elastic parameters than bulk materials, it is very easy to excite the internal vibrational degrees of freedom (phonon modes) when electrons are incident upon the molecule through a tunnel junction [10–13]. An important feature of the SMT is therefore its sensitivity to local molecular vibrations, which can have a profound impact on the transport properties. In fact, phonon-assisted tunneling peaks or steps have been experimentally observed in various single-molecule transistor systems.

Vibrations may also be important in some quantum dot (QD) systems, and consequently electron–phonon interactions in a QD have generated a great deal of interest in recent years as a model for SMTs. It has been experimentally demonstrated that the low-bias conductance of molecules is dominated by resonant tunneling through coupled electronic and vibration levels [14].

A common geometry used for transport studies in quantum dots consists of two leads weakly coupled to a QD via tunneling barriers. For the past decade, spin-dependent resonant tunneling through a QD, a small system characterized by discrete electronic states, coupled with a ferromagnet (F) and a superconductor (S) forming an F–QD–S system, has been subjected to considerable experimental and theoretical investigation [15–20]. It is found that Andreev reflection and spin-polarized transport can occur in an F–QD–S system. Cao *et al* [21] investigated the spin-dependent Andreev reflection in an F–QD–S system, for which the spin-flip scattering effect was considered. It is found that competition between the intradot spin-flip scattering and the tunneling coupling to the leads dominates the resonant behavior of the Andreev reflection conductance versus the gate voltage. However, effects of the phonon on Andreev reflection in an F–QD–S system has not yet been considered.

In addition to the mean-current properties, a detailed knowledge of transport in mesoscopic systems requires considering the noise properties. At zero temperature the shot noise is defined as the mean-square fluctuation of the current flowing through a given terminal. It is of great importance and interest because the spectrum of shot noise contains additional

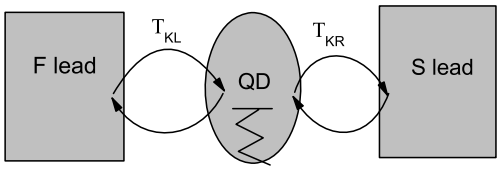

Figure 1. The quantum dot, with phonon modes and intradot spin–orbit interaction, is coupled to ferromagnetic and superconducting leads.

information about the interactions the conduction electrons undergo, beyond what can be obtained from the mean-current properties. In particular, it can be used to discern different mechanisms resulting in the same mean current [22–26].

In this paper, on the basis of the Green's function technique and canonical transformation of the electron–phonon interaction system, we study quantum transport through the SMT, as modeled by a QD, in the presence of finite bias and local electron–phonon interaction. Particular attention is paid to the effect of the electron–phonon coupling on the conductance and the shot noise.

The rest of this paper is organized as follows. In section 2, we introduce the model Hamiltonian and derive the formula for AR conductance and the shot noise by means of a nonequilibrium Green's function. In section 3, we present the numerical results and relevant discussion. Finally, a brief summary is given in section 4.

2. Model and formulae

As shown schematically in figure 1, our model system is a QD, with a single electron level, coupled to phonon modes in the QD as well as to two leads. For the sake of simplicity, with respect to the F-lead, we restrict ourselves exclusively to the election–phonon interaction (EPI) and the chemical potential.

The model Hamiltonian can then be expressed as

$$H = H_{\rm F} + H_{\rm S} + H_{\rm ph} + H_{\rm dot} + H_T. \tag{1}$$

The first three terms represent the noninteracting electron gas in the leads and the local vibration mode of the SMT, respectively:

$$H_{\rm F} = \sum_{k,\sigma} (\epsilon_{k\sigma} + \sigma M) f^\dagger_{k\sigma} f_{k\sigma}, \tag{2}$$

$$H_{\rm S} = \sum_{p,\sigma} \epsilon_{p\sigma} S^\dagger_{p\sigma} S_{p\sigma} + \sum_{p} (\Delta^* s^\dagger_{p\uparrow} s^\dagger_{p\downarrow} + \Delta s_{p\uparrow} s_{-p\downarrow}), \tag{3}$$

$$H_{\rm ph} = \omega_0 a^\dagger a, \tag{4}$$

where the $H_{\rm F}$ and $H_{\rm S}$ are the Hamiltonians for the F-lead and the S-lead, respectively. Under the mean-field approximation, the F-lead is characterized by an internal magnetic moment $\overline{M}$. The tilt angle between the magnetic moment and the F–QD interface has been chosen to be zero. The BCS Hamiltonian is adopted for the S-lead with Δ the energy gap. $H_{\rm ph}$ is the Hamiltonian for the phonon; ω_0 is the vibrational frequency of the molecule modeled by the QD and $a^\dagger(a)$ is the phonon creation (annihilation) operator.

The fourth term $H_{\rm dot}$ models the QD with the electron–phonon interaction and the intradot spin-flip scattering. Here, we focus on the phonon mode in the transport properties and the QD is controlled with gate voltage versus 2D electron gas: the electron–electron interaction is neglected. We denote the electron creation (annihilation) operators in the QD by $d^\dagger_\sigma(d_\sigma)$; σ is the spin index; λ is the electron–phonon coupling:

$$H_{\rm dot} = [\epsilon_d d^\dagger_\sigma d_\sigma + \lambda(a + a^\dagger)] d^\dagger d + R(d^\dagger_\uparrow d_\downarrow + d^\dagger_\downarrow d_\uparrow). \tag{5}$$

The spin-flip term in the $H_{\rm dot}$ comes from the spin–orbit interaction in the QD [21, 27, 28] and R is the scattering strength.

The last term H_T describes the tunneling between the QD and the F-lead (S-lead) with the tunneling matrix elements, $T_{k\sigma}(T_{p\sigma})$. We have assumed that the spin of the electrons is conserved during tunneling through the two side barriers of the QD:

$$H_T = \sum_{k,\sigma} (T_{k\sigma} f^\dagger_{k\sigma} d_\sigma + {\rm H.c}) + \sum_{p,\sigma} (T_{p\sigma} s^\dagger_{p\sigma} d_\sigma + {\rm H.c}). \tag{6}$$

Since we are interested in the case of strong electron–phonon interaction, it is appropriate to eliminate the electron–phonon coupling terms in the Hamiltonian by using a nonperturbative canonical transformation, i.e. $\overline{H} = e^s H e^{-s}$ with $S = (\lambda/\omega_0) d^\dagger_\sigma d_\sigma (a^\dagger - a)$. The transformed Hamiltonian is $\overline{H} = \overline{H}_{\rm ph} + \overline{H}_{\rm el}$, where the phonon part remains unchanged, while the electron part is reshaped into

$$\begin{aligned}\overline{H}_{\rm el} = & \sum_{k,\sigma} (\epsilon_{k\sigma} + \sigma M) f^\dagger_{k\sigma} f_{k\sigma} + \sum_{p,\sigma} \epsilon_{p\sigma} s^\dagger_{p\sigma} s_{p\sigma} \\ & + \sum_{p} (\Delta^* s^\dagger_{p\uparrow} s^\dagger_{-p\downarrow} + \Delta s_{p\uparrow} s_{-p\downarrow}) \\ & + \sum_{\sigma} \widetilde{\epsilon}_d d^\dagger_\sigma d_\sigma + R(d^\dagger_\uparrow d_\downarrow + d^\dagger_\uparrow d_\uparrow) \\ & + \sum_{k,\sigma} (\widetilde{T}_{k\sigma} f^\dagger_{k\sigma} d_\sigma + {\rm H.c.}) + \sum_{p,\sigma} (\widetilde{T}_{p\sigma} s^\dagger_{p\sigma} d_\sigma + {\rm H.c}).\end{aligned} \tag{7}$$

Because of the EPI, the energy level of the QD is renormalized to $\widetilde{\epsilon_d} \equiv \epsilon_d - g\omega_0$, where $g \equiv (\lambda/\omega_0)^2$, and the dressed tunneling matrix elements are transformed into $\widetilde{T}_{k\sigma} \equiv T_{k\sigma} X$, $\widetilde{T}_{p\sigma} \equiv T_{p\sigma} X$, where the phonon operator, $X \equiv \exp[-(\lambda/\omega_0)(a^\dagger - a)]$, arises from the canonical transformation of the particle operator, $e^s {\rm d} e^{-s} = {\rm d}X$.

However, it is a localized polaron that we are dealing with. It is reasonable to replace the operator X with its expectation value $\langle X\rangle = \exp[-g(N_{\rm ph} + 1/2)]$, where $N_{\rm ph}$ is the phonon population and can be expressed as $N_{\rm ph} = 1/[\exp(\beta\omega_0 - 1)]$, with $\beta = 1/k_\beta T$. Note that this is an important approximation made in the present paper and is valid only when the electron hopping between the leads and the QD is small compared to the EPI, i.e. $T_{k\sigma} \ll \lambda$. The tunneling terms between the QD and the F-lead are modified by a factor X, which describes the fact that the electron hopping is accompanied by a phonon cloud. Here, to avoid unnecessary complication, we assume that the leads are unaffected by the phonons. This means that we ignore a factor that results from the average of the X operator. This does not lead to a qualitative change in the tunneling currents [29–31].

The tunneling current can be expressed as [21]

$$J = J_{\rm N} + J_{\rm A}, \tag{8}$$

with

$$J_{\rm N} = \frac{e}{h}\int {\rm d}\omega\,[f_{\rm l}(\omega - eV) - f_{\rm r}(\omega)]\sum_{i=1,3}[G^{\rm r}_d\widetilde{\Gamma}_s G^{\rm r}_d\widetilde{\Gamma}_f]_{ii}, \tag{9}$$

and

$$J_{\rm A} = \frac{e}{h}\int {\rm d}\omega\,[f_{\rm l}(\omega - eV) - f_{\rm r}(\omega + eV)] \times \sum_{i=1,3}^{j=2,4} G^{\rm r}_{d,ij}(\widetilde{\Gamma}_f G^a_d\widetilde{\Gamma}_f)_{ji}, \tag{10}$$

where $f_{\rm l}(\omega)$ and $f_{\rm r}(\omega)$ are the Fermi-distribution functions in the left and right leads, respectively; $G^{\rm r}$ denotes the Fourier-transformed retarded Green's function; $\widetilde{\Gamma}_f$ is the tunneling coupling matrix between the QD and the F-lead; $J_{\rm N}$ is the normal tunneling current which is caused by the single quasihole transport and $J_{\rm A}$ is the Andreev reflection current. In the linear-response region, the normal tunneling conductance and AR conductance are obtained as follows:

$$G_{\rm N} = \frac{e^2}{h}\int {\rm d}\omega\,[-\partial f/\partial\omega]\sum_{i=1,3}[G^{\rm r}_d\widetilde{\Gamma}_s G^a_d\widetilde{\Gamma}_f]_{ii} \tag{11}$$

and

$$G_{\rm A} = \frac{2e^2}{h}\int {\rm d}\omega\,[-\partial f/\partial\omega]\sum_{i=1,3}^{j=2,4} G^{\rm r}_{d,ij}(\widetilde{\Gamma}_f G^a_d\widetilde{\Gamma}_f)_{ji}. \tag{12}$$

Since the normal linear conductance is zero ($G_{\rm N} = 0$), the total conductance G is equivalent to $G_{\rm A}$ at zero temperature. If only the Andreev reflection is taken into account, the shot noise spectrum has the following form [32]:

$$S = 8e^2\int\frac{{\rm d}E}{2\pi}T_r\{T_A[f(E-eV)(1-f(E+eV)) + f(E+eV)(1-f(E-eV))] - T_A^2[f(E-eV)-f(E+eV)]^2\}. \tag{13}$$

In the limit of low bias and zero temperature, the shot noise, S, simplifies into

$$S = \frac{4e^3V}{\pi}T_r[T_A(1-T_A)]. \tag{14}$$

Here we have defined T_A as the transmission coefficient matrix and can be expressed as the following form:

$$T_A = \begin{pmatrix} G^{\rm r}_{d,12}(\widetilde{\Gamma}_f G^a_d\widetilde{\Gamma}_f)_{21} & 0 & 0 & 0\\ 0 & G^{\rm r}_{d,14}(\widetilde{\Gamma}_f G^a_d\widetilde{\Gamma}_f)_{41} & 0 & 0\\ 0 & 0 & G^{\rm r}_{d,32}(\widetilde{\Gamma}_f G^a_d\widetilde{\Gamma}_f)_{23} & 0\\ 0 & 0 & 0 & G^{\rm r}_{d,34}(\widetilde{\Gamma}_f G^a_d\widetilde{\Gamma}_f)_{43}\end{pmatrix}. \tag{15}$$

Once the electron Green's functions are known, the conductance G and the shot noise S can be calculated by using equations (12) and (14). In the following, we calculate these Green functions. When the operator X is replaced by its expectation value, the Hamiltonian equation (7) is decoupled from the phonon operator, the original Green function for the electron in the QD can be expressed as [31]

$$G^{\rm r(a)}_{aa'} = \mp i\theta(\pm_i)\langle\{\widetilde{d}a(t), \widetilde{d}a'(0)\}\rangle_{\rm el}\langle X(t)X^\dagger(0)\rangle_{\rm ph} = \widetilde{G}^{\rm r(a)}_{aa'}(t)\langle X(t)X^\dagger(0)\rangle_{\rm ph}, \tag{16}$$

where $\widetilde{d}a(t) = {\rm e}^{{\rm i}\overline{H}_{\rm el}t}da{\rm e}^{-{\rm i}\overline{H}_{\rm el}t}$ and $X(t) = {\rm e}^{{\rm i}\overline{H}_{\rm ph}t}X{\rm e}^{-{\rm i}\overline{H}_{\rm ph}t}$. The renormalization factor is evaluated to be $\langle X(t)X^\dagger(t)\rangle_{\rm ph} = {\rm e}^{-\Phi(t)}$, where

$$\Phi(t) = (\lambda/\omega_0)^2[N_{\rm ph}(1-{\rm e}^{{\rm i}\omega_0 t}) + (N_{\rm ph}+1)(1-{\rm e}^{-{\rm i}\omega_0 t})]. \tag{17}$$

By using the identity ${\rm e}^{-\Phi(t)} = \Sigma_{-\infty}^{\infty}L_n{\rm e}^{-{\rm i}n\omega_0 t}$, the retarded Green's function can be expanded as

$$G^{\rm r}(\omega) = \sum_{n=-\infty}^{\infty}L_n\widetilde{G}^{\rm r}(\omega - n\omega), \tag{18}$$

where the index n stands for the number of phonons and L_n are coefficients depending on temperature and the strength of EPI. At finite temperature

$$L_n \equiv {\rm e}^{-g(2N_{\rm ph}+1)}{\rm e}^{n\omega_0\beta/2}I_n 2g\sqrt{N_{\rm ph}(N_{\rm ph}+1)}, \tag{19}$$

where $I_N(Z)$ is the n th Bessel function of complex argument. At zero temperature, L_n reduces to $L_n \equiv 0$ ($n < 0$) and $L_n \equiv {\rm e}^{-g}g^n/n!$ ($n \geqslant 0$). With the help of the equation of motion approach, the retarded Green's function for the dressed election can be evaluated analytically as

$$\widetilde{G}^{\rm r}(\omega) = \frac{1}{(\widetilde{g}^{\rm r})^{-1} - \widetilde{\Sigma}^{\rm r}}, \tag{20}$$

in which $\widetilde{g}^{\rm r}$ is the retarded Green's function for an isolated QD coupled with the phonon mode and $\widetilde{\Sigma}^{\rm r}$ is the self-energy matrix. The matrix $\widetilde{g}^{\rm r}$ can be easily obtained as ($\delta = +{\rm i}0^+$):

$$(\widetilde{g}^{\rm r})^{-1} = \begin{pmatrix} \omega - n\omega_0 - \widetilde{\epsilon}_d + \delta & 0 & 0 & 0\\ 0 & \omega - n\omega_0 + \widetilde{\epsilon}_d + \delta & 0 & 0\\ 0 & 0 & \omega - n\omega_0 - \widetilde{\epsilon}_d + \delta & 0\\ 0 & 0 & 0 & \omega - n\omega_0 + \widetilde{\epsilon}_d + \delta\end{pmatrix}. \tag{21}$$

For the F–QD–S system under study, $\widetilde{\Sigma}^{\rm r}$ can be written as $\widetilde{\Sigma}^{\rm r} = \widetilde{\Sigma}_R + \widetilde{\Sigma}^{\rm r}_f + \widetilde{\Sigma}^{\rm r}_s$, where the three terms refer to the energy contributions from intradot spin-flip and tunneling at the two leads as outlined below. The intradot spin-flip scattering contribution is conveniently expressed in terms of the self-energy $\widetilde{\Sigma}^R$ as

$$\widetilde{\Sigma}_R = \begin{pmatrix} 0 & 0 & R & 0\\ 0 & 0 & 0 & -R\\ R & 0 & & 0\\ 0 & -R & 0 & 0\end{pmatrix}, \tag{22}$$

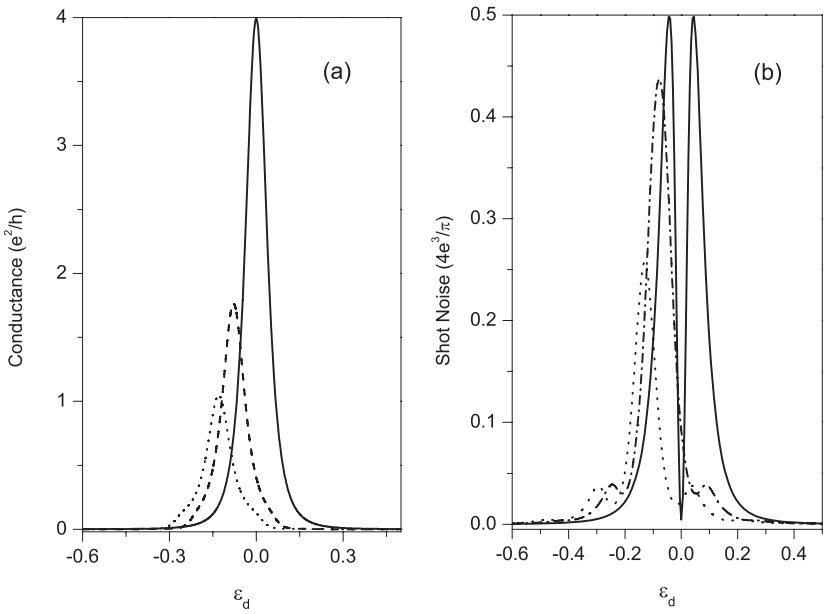

Figure 2. AR conductance (a) and shot noise (b) versus the energy level of the QD, with parameter $R = 0$. The electron–phonon couplings are taken to be: 0 for solid lines, $0.7\omega_0$ for dashed lines and $0.9\omega_0$ for dotted lines. The couplings between the QD and the leads are taken as $\Gamma_{f0} = \Gamma_{s0} = 0.1$.

where R is the scattering strength introduced above in equation (5).

The spin-dependent coupling between the QD and the F-lead can be described by the spin polarization P that specifies the F-lead magnetization. The spin-up and spin-down tunneling coupling strengths are defined as $\widetilde{\Gamma}_{f\uparrow} = \widetilde{\Gamma}_{f0}(1 + P)$ and $\widetilde{\Gamma}_{f\downarrow} = \widetilde{\Gamma}_{f0}(1 - P)$. The spin-averaged coupling strength $\widetilde{\Gamma}_{f0}$ denotes the tunneling coupling between the QD and the F-lead without internal magnetization and is defined by $\widetilde{\Gamma}_{f0} \equiv 2\pi\rho_f^n|\widetilde{T}_{k\sigma}|^2$ with $\widetilde{\rho}_f^n$ being the density of states for the F-lead without magnetization. Under the wide bandwidth approximation, the self-energy coupling to the F-lead is $\widetilde{\Sigma}_f^{\mathrm{r}} = -(\mathrm{i}/2)\widetilde{\Gamma}_f$, where $\widetilde{\Gamma}_f$ is the tunneling coupling matrix between the QD and the F-lead and is written as

$$\widetilde{\Gamma}_f = \widetilde{\Gamma}_{f0}\begin{pmatrix} (1+P) & 0 & 0 & 0 \\ 0 & (1-P) & 0 & 0 \\ 0 & 0 & (1-P) & 0 \\ 0 & 0 & 0 & (1+P) \end{pmatrix}. \tag{23}$$

The self-energy, $\widetilde{\Sigma}_s^{\mathrm{r}}$, takes into account the electron–phonon interaction due to the tunneling coupling between the QD and the S-lead, given by

$$\widetilde{\Sigma}_s^{\mathrm{r}} = -\frac{\mathrm{i}}{2}\widetilde{\rho}_s^{\mathrm{r}}(\omega)\widetilde{\Gamma}_{s0}\begin{pmatrix} 1 & -\frac{\Delta}{\omega-n\omega_0} & 0 & 0 \\ -\frac{\Delta}{\omega-n\omega_0} & 1 & 0 & 0 \\ 0 & 0 & 1 & \frac{\Delta}{\omega-n\omega_0} \\ 0 & 0 & \frac{\Delta}{\omega-n\omega_0} & 1 \end{pmatrix}, \tag{24}$$

where $\widetilde{\rho}_s^{\mathrm{r}}(\omega - n\omega_0)$ is the modified dimensionless BCS density of states:

$$\widetilde{\rho}_s^{\mathrm{r}}(\omega - n\omega_0) = \frac{|\omega - n\omega_0|\theta(|\omega - n\omega_0| - \Delta)}{\sqrt{(\omega - n\omega_0)^2 - \Delta^2}} + \frac{|\omega - n\omega_0|\theta(|\Delta - \omega - n\omega_0|)}{\sqrt{(\omega - n\omega_0)^2 - \Delta^2}}, \tag{25}$$

and $\widetilde{\Gamma}_{s0} = 2\pi\rho_s^n|\widetilde{T}_{p\sigma}|^2$ is the tunneling coupling strength between the QD and the S-lead. In $\widetilde{\rho}_s^n$, $\widetilde{\Gamma}_{s0}$ is the density of states when the superconducting lead is in the normal state.

3. Result and discussion

In this section, we numerically study the AR conductance and the shot noise at zero temperature. The energy level of the QD is controlled by the gate voltage, V_{G}, and is restricted in the range of the energy gap of the S-lead, $|-n\omega_0 + \widetilde{\epsilon}_d| < \Delta$ and $|-n\omega_0 + \widetilde{\epsilon}_d \pm R| < \Delta$. The Fermi energies of both the F-lead and S-lead are set to zero; the energy gap of the S-lead, Δ, is taken as the energy unit; the spin polarization is chosen as $P = 0.3$ and the frequency of the phonon mode is taken as $\omega_0 = 0.16$.

First, we take the coupling between the QD and the two leads to be symmetric, $\Gamma_{f0} = \Gamma_{s0} = 0.1$. The AR conductance and the shot noise are plotted in figure 2. It can be seen that, without the electron–phonon interaction, only one resonant conductance peak shows up as the Fermi energy matches the single level in the QD. When the electron energy matches the local level in the QD, a perfect AR process takes place and the value of the conductance reaches its maximum $4e^2/h$. However, in the presence of electron–phonon coupling, the overall conductance spectrum is shifted by $\Delta = \lambda^2/\omega_0$. As a result, the peaks of the conductance are located at $\varepsilon_d = -0.08, -0.13$. As the electron–phonon coupling increases, the heights of the main peaks decrease but the heights of the new resonant peaks increase.

In figure 2(b), the differential shot noise power exhibits two peaks when the electron–phonon interaction is not considered. The presence of two peaks can be explaining as arising from the fact that no noise is generated when the transmission probability is $T = 0$, or 1, while for $T = 0.5$,

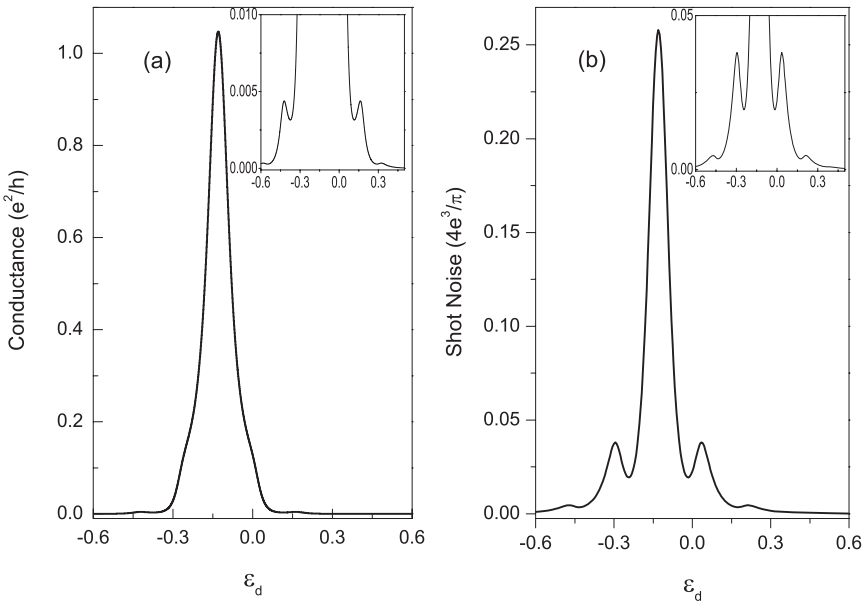

Figure 3. AR conductance (a) and shot noise (b) versus the energy level of the QD, with parameter $R = 0$. The couplings between the QD and the leads are taken as $\Gamma_{f0} = \Gamma_{s0} = 0.1$. The electron–phonon coupling is $0.9\omega_0$. Insets (a) and (b) are blowups.

maximal noise is generated. When the electron–phonon interaction is present, only one main shot noise peak appears, whose heights decrease as the phonon–electron coupling increases. On both sides of the main peaks, new satellite peaks appear whose heights increase as the electron–phonon coupling increases. We can see that the phonon peaks in shot noise are more remarkable than those in AR conductance.

The system we are ultimately modeling is a single molecule and it possesses much smaller elastic parameters. Under such circumstances, phonon emission and absorption readily occur, which lead to the appearance of satellite peaks. However, the intensity of the satellite peaks is much smaller than the main resonance peak because they derive from the emission of phonon modes. The height of the main peaks of the conductance and shot noise can be suppressed by the electron–phonon coupling.

In order to see the phonon peaks clearly, the dotted lines plotted in figure 2 are plotted alone in figure 3 with solid lines. It is found that new satellite resonant peaks appear in the curve of the conductance at $\epsilon_d = -\Delta \pm n\omega_0$ ($n = 1, 2, 3$). For this case, $\lambda = 0.9\omega_0$, $\Delta = 0.13$ (see the inset of figure 3(a) for clarity) phonon peaks appear at $\ldots, -0.45, -0.29, 0.03, 0.19, 0.35$, etc Comparing figure 3(b) with figure 3(a), we can see that, the phonon peaks in the shot noise are more profound than those in the conductance.

Take the coupling between the QD and the leads to be the same as that in figure 2. But with stronger spin-flip scattering $R = 0.1$, the curves of the conductance and the shot noise versus the energy level of the QD ϵ_d are plotted in figure 4. In figure 4(a), since $R > \Gamma_{s0}/2 + \Gamma_{f0}$, the two split levels have been separated from each other. At $\varepsilon_d = 0$, an almost vanishing spin-dependent energies emerges. Therefore, the AR conductance exhibits double resonant peaks.

When the electron–phonon coupling is not considered, the spin-splitting of the main peaks appears, while the curves for both the AR conductance and the shot noise are double peaks. When the electron–phonon coupling is considered, the new peaks show up on both sides of the main peaks. As the electron–phonon coupling increases, it is interesting to show that, in shot noise, i.e. when $\lambda = 0.8\omega_0$, a new peak shows up between the main peaks.

In figure 5, the coupling between the QD and the two leads is taken to be asymmetric with $\Gamma_{f0} = 0.02$ and $\Gamma_{s0} = 0.1$. Without electron–phonon coupling, the AR conductance can reach its maximum value of $4e^2/h$ at $\varepsilon_d = 0$, when the appropriate spin-flip scattering $R = 0.05$ appears. To explain this phenomenon, we define the ratio of the two tunneling coupling strengths $r = \Gamma_{s0}/\Gamma_{f0}$. The matching condition of the Fermi velocity [33], $\Gamma_{f\uparrow}\Gamma_{f\downarrow}$, is $P^2 + r^2 = 1$. When $\Gamma_{f0} = 0.02$, $\Gamma_{s0} = 0.1$, the matching of the Fermi velocity can never be satisfied. However, intradot spin scattering may yield an explanation. Spin-up and spin-down electrons can tunnel from the QD to the leads, which leads to resonance broadening of the two spin-coherent split levels by an amount Γ. Here the linewidth of the split levels, $\Gamma = (\Gamma_{f0} + \Gamma_{s0})$, delineates the distribution of the density of states. In figure 5, the AR conductance behaves as a single peak resonance because the spin-flip scattering strength is smaller than the broadening of the split levels. Once the spin-flip scattering strength reaches $R = \Gamma_{s0}/2$, the AR conductance can reach its maximum $4e^2/h$.

In the presence of electron–phonon coupling, phonon peaks appear and can be seen clearly in figures 5(c) and (d). It is found that phonon AR conductance peaks can be observed clearly. Correspondingly, the phonon shot noise peaks are more obvious. As the electron–phonon coupling increases, the splitting of the main shot noise peak decreases: when

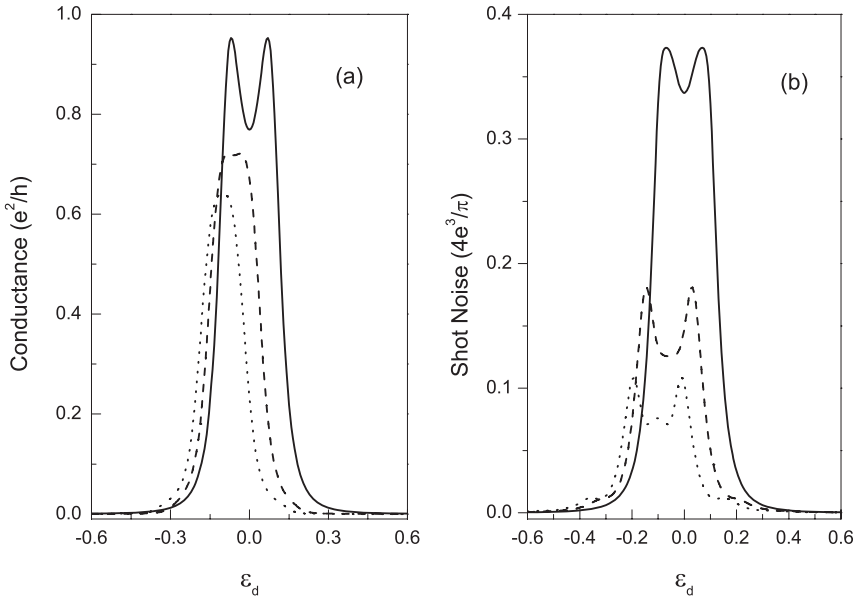

Figure 4. AR conductance (a) and shot noise (b) versus the energy level of the QD, with parameter $R = 0.1$. The electron–phonon couplings are taken as 0 for solid lines, $0.6\omega_0$ for dashed lines and $0.8\omega_0$ for dotted lines. The couplings between the QD and the leads are taken as $\Gamma_{f0} = \Gamma_{s0} = 0.1$.

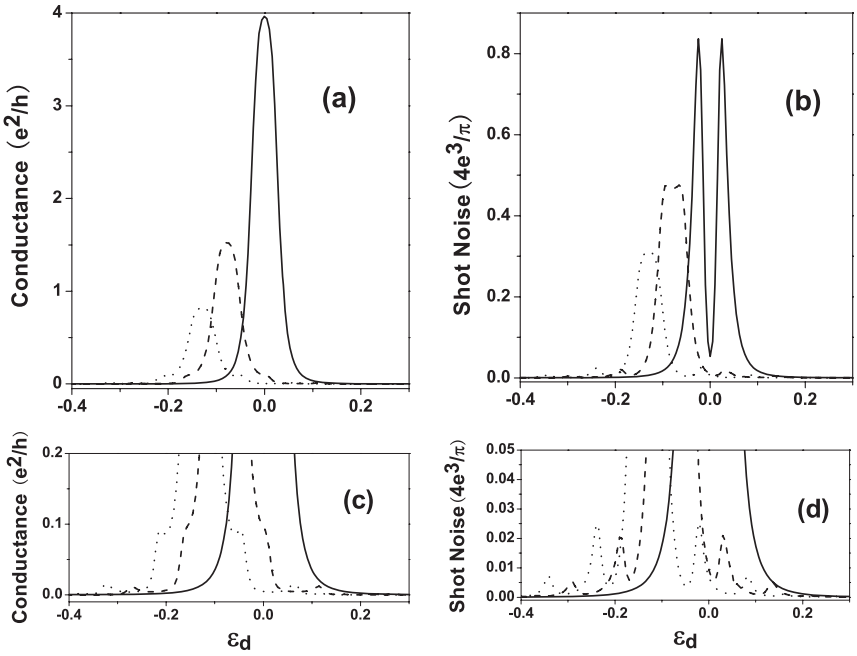

Figure 5. AR conductance (a) and shot noise (b) versus the energy level of the QD, with parameter $R = 0.05$. The electron–phonon couplings are taken as 0 for solid lines, $0.5\omega_0$ for dashed lines and $0.8\omega_0$ for dotted lines. The couplings between the QD and the leads are taken as $\Gamma_{f0} = 0.02$ and $\Gamma_{s0} = 0.1$. (c) and (d) are blowups of (a) and (b), respectively.

$\lambda = 0.8\omega_0$, the main shot noise peaks change into a single peak from double peaks.

The curves of the conductance and the shot noise versus the energy level of the QD ϵ_d are plotted in figure 6, with a stronger spin-flip scattering, $R = 0.1$, and an asymmetrical coupling between the QD and the leads. In figure 6(a), when the electron–phonon interaction does not exist, the AR conductance appears as a symmetric double peak resonance when the spin-flip scattering is sufficiently enhanced, $R = 0.1$. In the presence of electron–phonon coupling, the AR conductance and the shot noise varies more complicatedly. New satellite peaks appear on both sides of the main resonant double peaks. With increasing electron–phonon coupling the heights of the new resonant peaks increase. In figure 6(b), when the electron–phonon interaction does not exist, the shot noise exhibits a resonant double peak. In the presence of electron–phonon coupling, on both sides of the main resonant, new double peaks emerge. The new

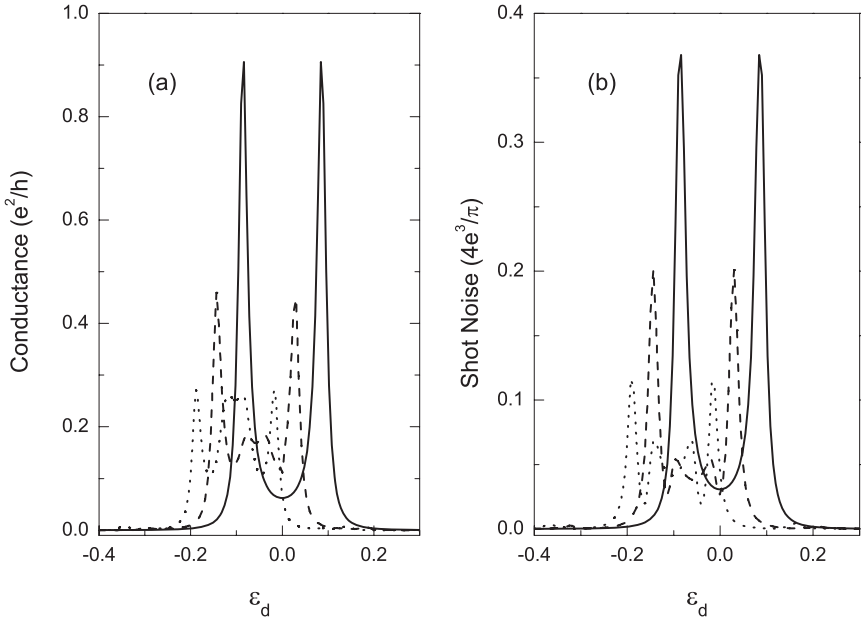

Figure 6. AR conductance (a) and shot noise (b) versus the energy level of the QD, with parameter $R = 0.1$. The electron–phonon couplings are taken as 0 for solid lines, $0.6\omega_0$ for dashed lines and $0.8\omega_0$ for dotted lines. The couplings between the QD and the leads are taken as $\Gamma_{f0} = 0.02$ and $\Gamma_{s0} = 0.1$.

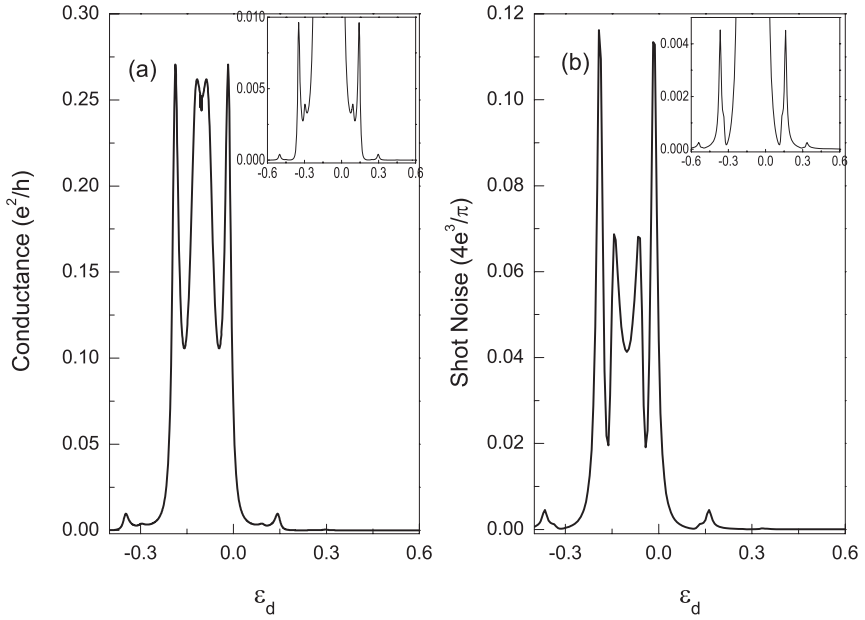

Figure 7. AR conductance (a) and shot noise (b) versus the energy level of the QD, with parameter $R = 0.1$. The electron–phonon coupling is $0.8\omega_0$. The couplings between the QD and the leads are taken as $\Gamma_{f0} = 0.02$ and $\Gamma_{s0} = 0.1$. Insets (a) and (b) are blowups.

phonon peaks can be seen more clearly. Moreover, new double resonant peaks appear in the middle of the main resonant double peaks in both the AR conductance and the shot noise, because the spin-flip scattering splittings take effect on the satellite peaks resulting from the electron–phonon interaction. The heights and the splittings of the new resonant double peaks increase with increasing electron–phonon coupling.

In order to show the phonon peaks more clearly, the curves of the shot noise and the conductance (plotted with dotted lines in figure 6) are plotted alone in figure 7. The phonon peaks in conductance are located exactly at $\varepsilon_d = -\Delta \pm n\omega_0 \pm R$. For this case, see the inset of figure 7(a) for clarity. When $\lambda = 0.8\omega_0$, the phonon peaks are located at $\ldots, -0.322, -0.162, 0.158, 0.318$, etc. The peaks due to the spin-flip scattering appear at $\varepsilon_d = -\Delta \pm R$, that is, $-0.204, 0.004$. We can also see the new double resonant peaks clearly in the conductance and the shot noise and the splittings of them can be seen to be more profound in the shot noise than in the conductance.

4. Conclusion

In summary, on the basis of the nonequilibrium Green's function method and a canonical transformation of the electron–phonon interaction, we have studied the influence of the electron–phonon interaction on the AR conductance and the shot noise when electrons tunnel through a quantum dot coupled with ferromagnetic and superconductor leads. The intradot spin-flip interaction is also taken into account. It is found that the AR conductance behaves as a single peak resonance when the spin-flip scattering strength is smaller than the broadening of the split levels. However, the AR conductance appears as a symmetric double peak resonance when the spin-flip scattering is sufficiently enhanced. In the presence of the electron–phonon interaction, new satellite resonant peaks appear and they are located exactly on the number of the phonon frequency. Moreover, the peak height is sensitive to the electron–phonon coupling. Even when the electron–phonon coupling is weak, the shot noise spectrum shows the phonon mode peaks clearly, but in AR conductance the phonon mode peaks are very weak. Spin-flip appears not only in the main AR peaks but also in the satellite peaks which result from the presence of the electron–phonon interaction.

Acknowledgments

This work was supported by the National Natural Science Foundation of China (grant no. 10674040) and the Hebei Province Natural Science Foundation (grant no. A2007000227).

References

[1] Poirier W, Mailly D and Sanquer M 1997 *Phys. Rev. Lett.* **79** 2105
[2] Morpurgo A F, Van Wees B J, Klapwijk T M and Borghs G 1997 *Phys. Rev. Lett.* **79** 4010
[3] Upadhyay S K, Palanisami A, Louie R N and Buhrman R A 1999 *Phys. Rev. Lett.* **81** 3124
[4] Guéron S, Deshmukh M M, Myers E B and Ralph D C 1999 *Phys. Rev. Lett.* **83** 4148
[5] Park H, Park J, Lim A K L, Anderson E H, Alivisatos A P and McEuen P L 2000 *Nature* **407** 57
[6] Park J, Pasupathy A, Goldsmith J, Chang C, Yaish Y, Petta J, Rinkoski M, Sethna J, Abruna H and McEuen P 2002 *Nature* **417** 722
[7] Liang W, Shores M, Bockrath M, Long J and Park H 2002 *Nature* **417** 725
[8] Kubatkin S, Dainlov A, Hjort M, Cornil J, Brédas J-L, Stuhr-Hansen N, Hedegard P and Bjornholm T 2003 *Nature* **425** 698
[9] Pasupathy A N, Bialczak R C, Martinek J, Grose J E, Donev L A K, McEuen P L and Ralph D C 2004 *Science* **306** 86
[10] Reed M A, Zhou C, Muller C J, Burgin T P and Tour J M 1997 *Science* **278** 252
Chen J, Reed M, Rawlett A and Tour J 1999 *Science* **286** 1550
[11] Ventra M D, Kim S G, Pantelides S T and Lang N D 2001 *Phys. Rev. Lett.* **86** 288
[12] Park H, Lim M, Anderson E, Allvisatos A and Euen P M 2000 *Nature* **407** 57
[13] Yu L H and Natelson D 2004 *Nano Lett.* **4** 79
[14] Zhitenev N B, Meng H and Bao Z 2002 *Phys. Rev. Lett.* **88** 226801
[15] De Jong M J M and Beenakker C W J 1995 *Phys. Rev. Lett.* **74** 1657
[16] Soulen R J *et al* 1998 *Science* **282** 85
[17] Žutić I and Sarma A D 1999 *Phys. Rev.* B **60** R16 322
[18] Žutić I and Valls O T 1999 *Phys. Rev.* B **60** 6320
[19] Meseryvey R and Tedrow P M 1994 *Phys. Rep.* **238** 173
[20] Blonder G E, Tinkam M and Klapwijk T M 1982 *Phys. Rev.* B **25** 4515
[21] Cao X, Shi Y, Song X and Zhou S 2004 *Phys. Rev.* B **70** 235341
[22] Blanter Y M and Buttiker M 2000 *Phys. Rep.* **336** 1
[23] Büttiker M 1992 *Phys. Rev.* B **46** 12485
[24] Reznikov M, Heiblum M, Shtrikman H and Mahalu D 1995 *Phys. Rev. Lett.* **75** 3340
[25] Nagaev K E 1998 *Phys. Rev.* B **57** 4628
[26] Wang B G, Wang J and Guo H 2003 arXiv:cond-mat/03050066
[27] Khaetskii A V and Nazarov Y V 2000 *Phys. Rev.* B **61** 12639
Khaetskii A V 2001 *Physica* E **10R** 27
[28] Zhang P, Xue Q K, Wang Y P and Xie X C 2002 *Phys. Rev. Lett.* **89** 286803
[29] Lundin U and Mckenzie R H 2002 *Phys. Rev.* B **66** 075303
[30] Mahan G D 1990 *Many-Particle Physics* 2nd edn (New York: Plenum) pp 285–324
[31] Chen Z, Lu R and Zhu B 2005 *Phys. Rev.* B **71** 165324
[32] Peng J, Wang B and Xing D Y 2005 *Phys. Rev.* B **71** 214523
[33] Zhu Y, Sun Q F and Lin T H 2001 *Phys. Rev.* B **65** 024516